NASA/TM—2010-216090

Ultrasonic Phased Array Inspection for an Isogrid Structural Element With Cracks

D.J. Roth and R.P. Tokars
Glenn Research Center, Cleveland, Ohio

R.E. Martin
Cleveland State University, Cleveland, Ohio

R.W. Rauser
The University of Toledo, Toledo, Ohio

J.C. Aldrin
Computational Tools, Inc., Gurnee, Illinois

E.J. Schumacher
Magsoft Corporation, Ballston Spa, New York

March 2010

NASA STI Program . . . in Profile

Since its founding, NASA has been dedicated to the advancement of aeronautics and space science. The NASA Scientific and Technical Information (STI) program plays a key part in helping NASA maintain this important role.

The NASA STI Program operates under the auspices of the Agency Chief Information Officer. It collects, organizes, provides for archiving, and disseminates NASA's STI. The NASA STI program provides access to the NASA Aeronautics and Space Database and its public interface, the NASA Technical Reports Server, thus providing one of the largest collections of aeronautical and space science STI in the world. Results are published in both non-NASA channels and by NASA in the NASA STI Report Series, which includes the following report types:

- TECHNICAL PUBLICATION. Reports of completed research or a major significant phase of research that present the results of NASA programs and include extensive data or theoretical analysis. Includes compilations of significant scientific and technical data and information deemed to be of continuing reference value. NASA counterpart of peer-reviewed formal professional papers but has less stringent limitations on manuscript length and extent of graphic presentations.

- TECHNICAL MEMORANDUM. Scientific and technical findings that are preliminary or of specialized interest, e.g., quick release reports, working papers, and bibliographies that contain minimal annotation. Does not contain extensive analysis.

- CONTRACTOR REPORT. Scientific and technical findings by NASA-sponsored contractors and grantees.

- CONFERENCE PUBLICATION. Collected papers from scientific and technical conferences, symposia, seminars, or other meetings sponsored or cosponsored by NASA.

- SPECIAL PUBLICATION. Scientific, technical, or historical information from NASA programs, projects, and missions, often concerned with subjects having substantial public interest.

- TECHNICAL TRANSLATION. English-language translations of foreign scientific and technical material pertinent to NASA's mission.

Specialized services also include creating custom thesauri, building customized databases, organizing and publishing research results.

For more information about the NASA STI program, see the following:

- Access the NASA STI program home page at *http://www.sti.nasa.gov*

- E-mail your question via the Internet to *help@sti.nasa.gov*

- Fax your question to the NASA STI Help Desk at 443–757–5803

- Telephone the NASA STI Help Desk at 443–757–5802

- Write to:
  NASA Center for AeroSpace Information (CASI)
  7115 Standard Drive
  Hanover, MD 21076–1320

NASA/TM—2010-216090

Ultrasonic Phased Array Inspection for an Isogrid Structural Element With Cracks

D.J. Roth and R.P. Tokars
Glenn Research Center, Cleveland, Ohio

R.E. Martin
Cleveland State University, Cleveland, Ohio

R.W. Rauser
The University of Toledo, Toledo, Ohio

J.C. Aldrin
Computational Tools, Inc., Gurnee, Illinois

E.J. Schumacher
Magsoft Corporation, Ballston Spa, New York

National Aeronautics and
Space Administration

Glenn Research Center
Cleveland, Ohio 44135

March 2010

Acknowledgments

CIVA software is developed by the French Atomic Energy Commission (CEA)
and is distributed and supported by Magsoft Corporation.

Level of Review: This material has been technically reviewed by technical management.

Available from

NASA Center for Aerospace Information
7115 Standard Drive
Hanover, MD 21076–1320

National Technical Information Service
5301 Shawnee Road
Alexandria, VA 22312

Available electronically at http://gltrs.grc.nasa.gov

Ultrasonic Phased Array Inspection for an Isogrid Structural Element With Cracks

D.J. Roth and R.P. Tokars
National Aeronautics and Space Administration
Glenn Research Center
Cleveland, Ohio 44135

R.E. Martin
Cleveland State University
Cleveland, Ohio 44115

R.W. Rauser
The University of Toledo
Toledo, Ohio 43606

J.C. Aldrin
Computational Tools, Inc.
Gurnee, Illinois 60031

E.J. Schumacher
Magsoft Corporation
Ballston Spa, New York 12020

Abstract

In this investigation, a T-shaped aluminum alloy isogrid stiffener element used in aerospace applications was inspected with ultrasonic phased array methods. The isogrid stiffener element had various crack configurations emanating from bolt holes. Computational simulation methods were used to mimic the experiments in order to help understand experimental results. The results of this study indicate that it is at least partly feasible to interrogate this type of geometry with the given flaw configurations using phased array ultrasonics. The simulation methods were critical in helping explain the experimental results and, with some limitation, can be used to predict inspection results.

Introduction

Integrally-stiffened structures, such as isogrid panels and shells (an example of which is shown in Fig. 1(a)) are commonly used in aerospace applications (Ref. 1). These self-stiffened structures are effective where low mass, as well as overall stiffness and strength are desired. Common applications include propellant tanks and lower stage structures of space launch vehicles. If fasteners are used to attach internal structure through the isogrid structure, cracks may originate from the fastener holes. These cracks can then propagate through the exterior wall surface, which can be catastrophic for applications such as pressurized propellant tanks where the isogrid wall must contain the propellant and maintain pressure. Such cracks are not observable from the external surface of the structure until after propagation through the exterior wall, and often the interior surface is inaccessible for inspection. Thus, methods for inspection of these holes from the exterior isogrid surface are highly desirable.

The T-shaped element shown in Figure 1(b) is a stiffening subcomponent of an integrally-stiffened structure. The upper surface labeled inspection side represents the outerwall of the isogrid, which would be the pressure barrier for a propellant tank application. The rib is the interior stiffening component. The holes represent points where internal structure would be fastened, and cracks that might form at the fastener (e.g., bolt) holes are illustrated. The goal of the inspection would be to detect these cracks from

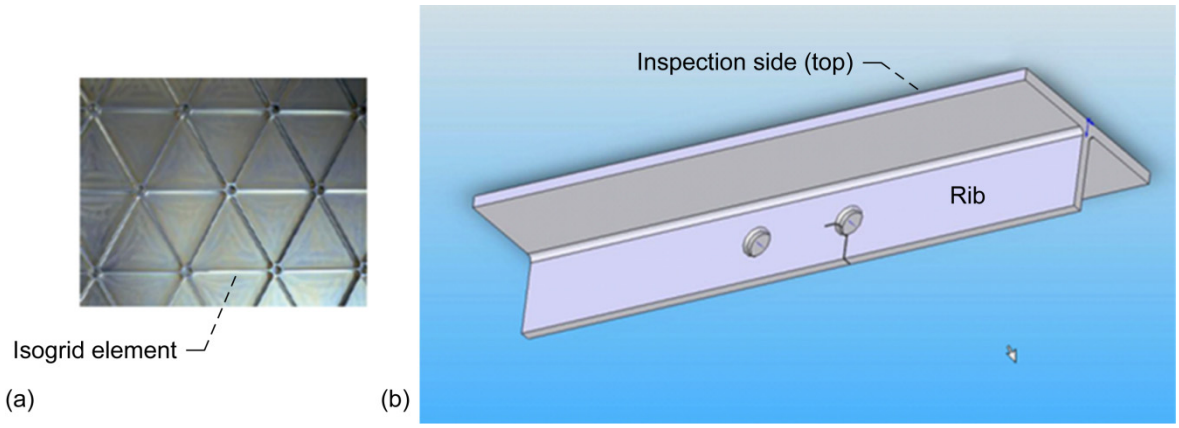

Figure 1.—(a) Integrally-stiffened isogrid shell structure. (b) Solid model of isogrid stiffener element with bolt holes and showing possible crack configurations.

the exterior (top) or inspection side. Ultrasonic inspection is a natural NDE candidate for internal surface flaw detection from external surfaces. The geometry of the isogrid element does not easily lend itself to ultrasonic inspection since the body, or rib, of the structure is a narrow element perpendicular to and projecting from the top. UT inspection could be implemented from the exterior surface, but would likely have limited detection capability of primary cracks due to "shadowing" from the rib/stiffener fasteners for cracks in certain orientations (Ref. 2). Nevertheless, ultrasonic inspection is still worth considering in this case for a number of reasons. These include the study of bulk wave ultrasonic propagation through thin elements for practical inspection, and the use of phased array ultrasonics (Refs. 3 to 6) for this type of an application.

Ultrasonic phased array transducers are made of multiple crystals that are electronically pulsed in a sequence using a specified delay between pulses to create electronic scanning, beam steering, and/or focusing capability. Ultrasonic phased array inspection is gaining wide acceptance and has many advantages over conventional A-scan inspection. These advantages include the ability to perform scanning with no mechanical movement, the ability to perform angular (sectorial) scans and dynamic focusing without setup alteration (thus more feasible and efficient for inspecting complex shapes and difficult-to-inspect areas), two-dimensional visualization of results, and similar portability to A-scan equipment.

Ultrasonic phased array inspection results can be difficult to understand due to the complexity of angular ultrasound compounded by multiple transducer element excitation. Computational simulation of the inspection, or "virtual" inspection, would thus be very desirable to aid in understanding of experimental results. Additionally, if such simulation methods are proven accurate, they can then be used to predict in a rapid and cost-effective fashion the feasibility and potential outcome of inspections under consideration (Ref. 7).

In this investigation, isogrid test samples with various simulated crack configurations emanating from bolt holes were inspected using an ultrasonic phased array method. In concert with actual inspections, computational simulations mimicking the actual inspection were performed within the limitations of the software. The results are presented from the simplest case (only bolt hole with no flaws) to more complex cases where various configurations of flaws are emanating from a bolt hole.

Test Samples

Four aluminum 2014 alloy isogrid stiffener element samples were manufactured with notches emanating from bolt holes (Fig. 2(a)). The sample length is 15.24 cm. The top of the "T" is 5.08 cm in width. The thicknesses of the rib and top are 0.27 and 0.29 cm, respectively. A fillet radius of 0.15 cm connects the rib with the top. Notch length and thickness was 0.64 and 0.27 cm (equal to that of the isogrid rib thickness), respectively.

Figure 2.—(a) The General Electric (GE) Phasor XS portable ultrasonic flaw detector. (b) Phased array probe positioned on the external side (top) of the isogrid test part.

Phased Array Ultrasonic Method

The General Electric (GE) Phasor XS portable ultrasonic flaw detector (Fig. 2(a)) was used for the actual test part inspection. The phased array probes consisted of a transducer on top of a wedge. The transducer employed was a 32 crystal-element linear phased array type with 5 MHz flat focus. The total aperture was 16 by 10 mm. The element width was approximately 0.45 mm and the gap (pitch) between elements was approximately 0.05 mm. Only 16 of the 32 elements are active at any one time as only 16 pulser-receivers are available in the instrument. The active aperture area was thus 8 by 10 mm. The transducer was attached to a wedge made of Rexolite plastic with incidence angle of approximately 36°. Figure 2(b) shows a photograph of the probe sitting on the top of the isogrid test sample in a typical inspection scenario. The probe was horizontally positioned so that the side of the wedge was perpendicular to the axis of the bolt holes. Depending on the specific flaw configurations, the probe might be moved horizontally by hand in either direction from a baseline position to achieve prominent indications. Generally, the edge of the probe wedge was located near either edge of the bolt hole (see Fig. 2(b)). Sectorial scans with inspection/refraction ranges of 20° to 50° (shear wave) and 40° to 70° (shear wave) were performed. Note that for the former range, longitudinal waves are predicted to be present up to $\theta_S = 29.2°$ (shear wave angle of refraction) as determined from Snell's law (Ref. 8):

$$\mathrm{Sin}\,\theta_L / V_L = \mathrm{Sin}\,\theta_s / V_s \tag{1}$$

using measured values of shear wave velocity ($V_S = 0.320$ cm/μsec) and longitudinal wave velocity ($V_L = 0.656$ cm/μsec) for aluminum 2014, and setting $\mathrm{Sin}\theta_L = 1$ (θ_L = angle of refraction for longitudinal waves = 90°). (See section entitled "*Additional Ultrasonic Testing*")

The situation of having longitudinal waves present in addition to shear waves during an angled inspection is actually an undesirable one and probably not often used in practice. It is a complicated enough scenario just using one mode due to all of the resulting mode conversions that occur for reflections from nonperpendicular incident ultrasonic waves off of internal boundaries. However, because of the geometry of the notches with respect to the bolt holes and probe, it was desired to at least attempt lower inspection angles.

Additional Ultrasonic Testing

The 5 MHz shear and longitudinal wave ultrasonic velocity measurements were performed on one of the isogrid stiffener element test samples using a precision contact ultrasonic method (Ref. 9). The shear and longitudinal wave velocity values for the test sample were measured to be 0.320 and 0.656 cm/μsec, respectively.

Ultrasonic Simulation

In this investigation, CIVA 9.1a software was utilized to model the phased array ultrasonic inspection of the isogrid stiffener element. The CIVA software allows bulk wave beam field predictions using the elastodynamics pencil method, and flaw response predictions using Kirchhoff, GTD or Born models for beam/flaw interaction (Refs. 10 to 17). CIVA can model many bulk wave inspection scenarios including A-scan, B-scan, C-scan, and S-scan (sectorial scan). The software has many powerful options available including the ability to compute delay laws for phased array ultrasonic setups (Refs. 6 and 18) and the ability to overlay resulting beam profiles and beam/flaw responses onto the model of the part. Beam profile visualizations show ultrasound propagation directions, focal spot locations, modes, and beam widths. Components requiring flaw response predictions need to be chosen from the directory of pre-existing specimen shapes, imported as two-dimensional DXF files, or drawn in two-dimensional profile in the computer-aided-design (CAD) facility included in the CIVA software. After the two-dimensional profile is created or imported, it is subsequently extruded to create the three-dimensional solid model. (Three-dimensional solid models can be imported into CIVA, but currently only for beam field predictions.) Materials can be added from the existing CIVA material library, or defined by the user. Subsequently, flaws can be added from the existing CIVA flaw library or imported from/created in a CAD facility. Reference 5, and Figure 3, explain the simulation process steps in more detail.

The geometry of the isogrid test sample presents somewhat of a problem for the two-dimensional CAD facility in CIVA with regards to predicting flaw response. If one considers the initial two-dimensional geometries prior to extrusion for the isogrid sample three-dimensional solid model, there are two possibilities. The first two-dimensional geometry that can be considered is that of a “T” shape. In this

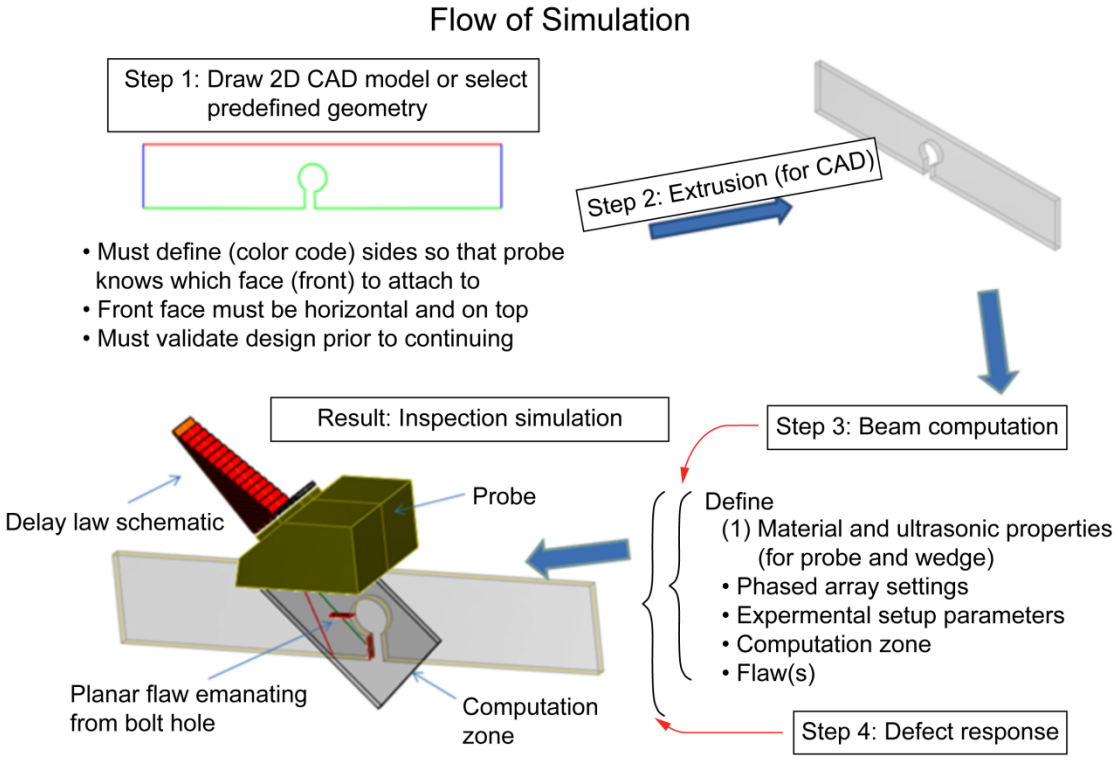

Simulation steps: (1) Two-dimensional profile of the isogrid test sample is drawn in the CIVA CAD facility. (2) The profile is extruded to create a three-dimensional solid model. (3) The material, setup, and flaw parameters are defined to create the inspection simulation. Beam computation can proceed after extrusion. (4) Defect response can proceed after flaw(s) is defined and inserted into the structure.

Figure 3.—Simulation steps for the isogrid test sample.

case, the “T” shape of selected dimensions can be extruded longitudinally the appropriate length so that it creates the isogrid three-dimensional solid model. Call this the “T” configuration. However, in this situation, the bolt hole cannot be incorporated into the initial two-dimensional “T” and still account for interaction between the bolt hole and the flaw. (A hole can be incorporated into the “T” three-dimensional solid model configuration after extrusion by addition of a circular flaw which is actually done in this investigation to consider ultrasonic reflection from just the bolt hole. But addition of the bolt hole and additional flaws results in improper modeling of the ultrasonic interactions between the bolt hole and the planar flaw simulating the notch/crack. CIVA is not configured to model flaw-flaw interaction. If backwall reflections between the holes and flaws are not expected to be significant, then the modeling is accurate when the holes are drawn as flaws.)

The second two-dimensional geometry that can be considered is a rectangle that has a discontinuous hole in it for the purpose of connecting the hole to (part of) the backwall (bottom surface). CIVA requires the bolt hole to be drawn as part of the backwall to correctly model the ultrasonic interaction between the bolt hole and the notches, including any corner trap effects between the hole and flaw. Extrusion can thus take place in the thickness direction which results in a three-dimensional solid model with bolt hole. However, in this case, the top of the “T” is missing so that the ultrasonic probe is actually modeled as sitting on top of the thickness. This “I” configuration does not accurately simulate the actual inspection condition, but it was the only choice for simulation using CIVA for flaw response that includes interactions with the bolt hole and backwall. For the beam profile, both “I” and “T” geometries and subsequent extrusions were performed in order to compare beam profiles for both solid models.

For the CAD modeling in the CIVA two-dimensional CAD facility, all sides were color-coded as front, back, side, and interface so that the ultrasonic probe attached itself properly, and the beam field and flaw response predictions were calculated correctly. Only one material zone needed to be defined since the entire part was the same material. (This is in contrast to the study of Reference 5 where the part was divided into four distinct zones since weld material was different from base material.) As already noted, the (discontinuous) hole was made a part of the backwall as required to correctly model interaction between surfaces and flaws. The CIVA software has interface screens for the user to describe the transducer crystal element characteristics and geometry, phased array crystal assembly, inspection/scan parameters, wedge material and geometry, test sample material and geometry, flaw material and geometry, and computation parameters. The model parameters selected matched closely with actual experimental parameters. The notch/crack was modeled as a planar flaw. The flaws were added after the CAD model was completed.

The “half-skip” sound path interaction with the flaw was chosen in the computation parameters. When the half-skip option is chosen, beam-flaw interactions that are in the direct sound path from the probe to the flaw and vice-versa are considered. Additionally, waves incident on flaws after reflection off the backwall and reflections from the flaws off the backwall towards the probe are also taken into account. This option therefore enables the computation of corner (trap) echoes, or more generally, echoes resulting from the inward and/or outward reflection off flaws via the backwall. Therefore, for the half-skip option, the echoes taken into account can include the specular reflections, tip diffractions, and corner-like echoes.

Backwall echoes were included in the computation (surface echoes were not included so as not to clutter up the displays). Shadowing was included since in some of the flaw configurations, the shadowing effect of a flaw onto the echo-response from other flaws or from component geometry might need to be considered. Sectorial scans were simulated using similar angles for the experimental phased array. A computation zone was selected that encompassed the bolt hole area. Computation accounted for mode conversion, but did not account for material noise or attenuation in this study. These are options which can be modeled, but increase computation time. The computed delay laws controlling the sector scan were not compared with the actual delay laws for the instrument because the latter are not readily exportable from the instrument. The overall flaw response calculation computes the signal received by the probe as the summation of individual contributions for the various resulting wave modes. The computation mode was two-dimensional—the planar flaw was meshed along its profile vertically-

perpendicular to the sound beam projection. The Kirchhoff approximation (Ref. 19) was used in the flaw response calculations. The Kirchhoff approximation assumes that the elastic wave is entirely scattered by the flaw. The flaw is meshed and the wave scattered by the flaw is the product of amplitude and time-dependent functions of incident wave and complex scattering coefficient at each meshed location. The Kirchhoff approximation relies on the assumption that each point at the flaw surface contributes as if it was part of an infinite plane (no interaction with neighboring points). The Kirchhoff approximation is assumed to give accurate results for flaws providing specular or near specular reflection over planar or volumetric flaws. Quantitative error is expected to increase when the scattered direction moves away from the specular direction.

The Kirchhoff approximation is a high frequency approximation, valid when $2\pi a/\lambda >> 1$ (i.e., when the flaw length (a) is significantly greater than the wavelength (λ)). In this case, the aluminum alloy has a shear wave velocity around 0.320 cm/μsec and at a frequency of 5 MHz, the wavelength is approximately 0.64 mm (using wavelength = velocity/frequency). Then, 2π*2.64 mm/0.64 mm ~26 (planar flaw length of about four times larger than the ultrasonic wavelength) which satisfies the Kirchhoff criterion.

Beam Profile Simulation Results

Figure 4 shows beam profile results for several shear wave inspection angles for the extruded "T" solid model. The beam profiles are overlaid on top of the solid model. Focusing on the computation zone within the test sample, one can see ultrasonic propagation directions, focal spot locations, modes, and beam widths. The single red and green lines show the center lines for shear and longitudinal wave propagation, respectively. It can be seen that at inspection angles (shear wave) up to around 29°, both shear and longitudinal waves are shown to be present.

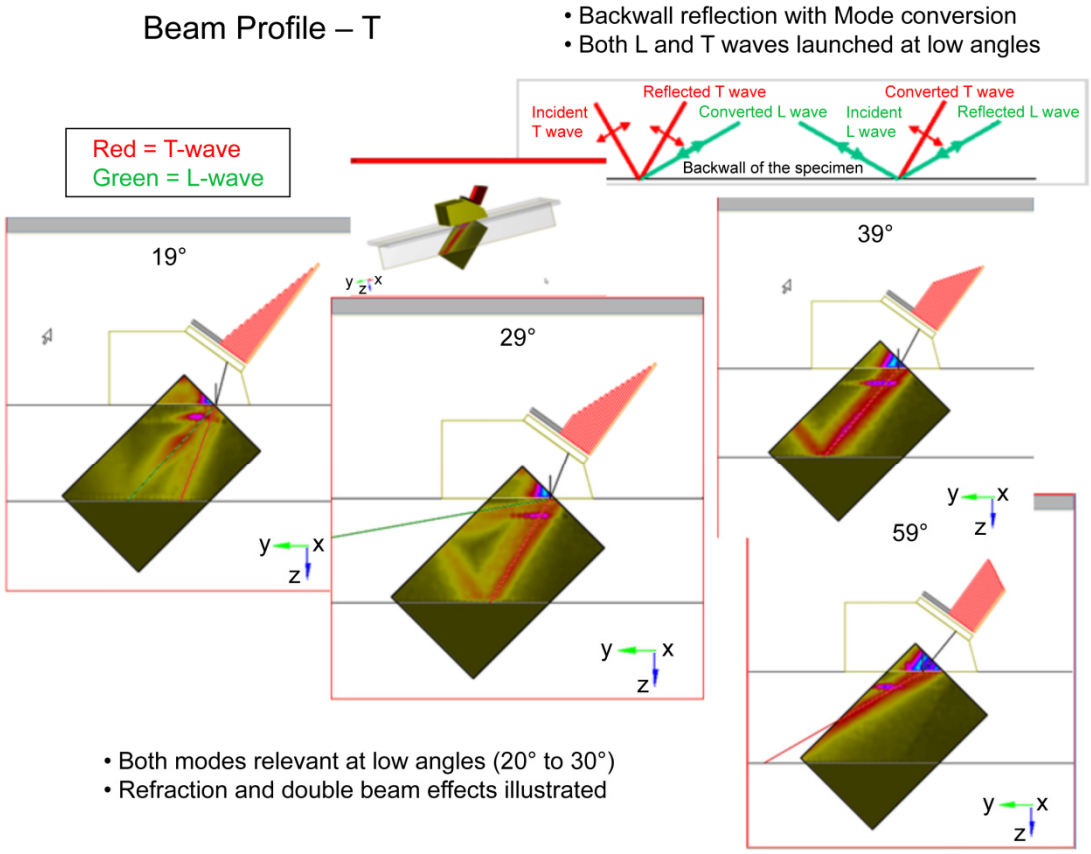

Figure 4.—Beam profile results for several shear wave inspection angles for the extruded "T" solid model.

Figure 5 shows a comparison of the beam profiles for the “I” and “T” solid models indicating some differences in resulting beams within the sample. This is most likely due to the additional ultrasonic interactions between the fillet area and ribwall for the “T” model. This interaction is explained by viewing Figure 6 which shows the likely paths of beams (and reflections off of a bolt hole) when a fillet is present.

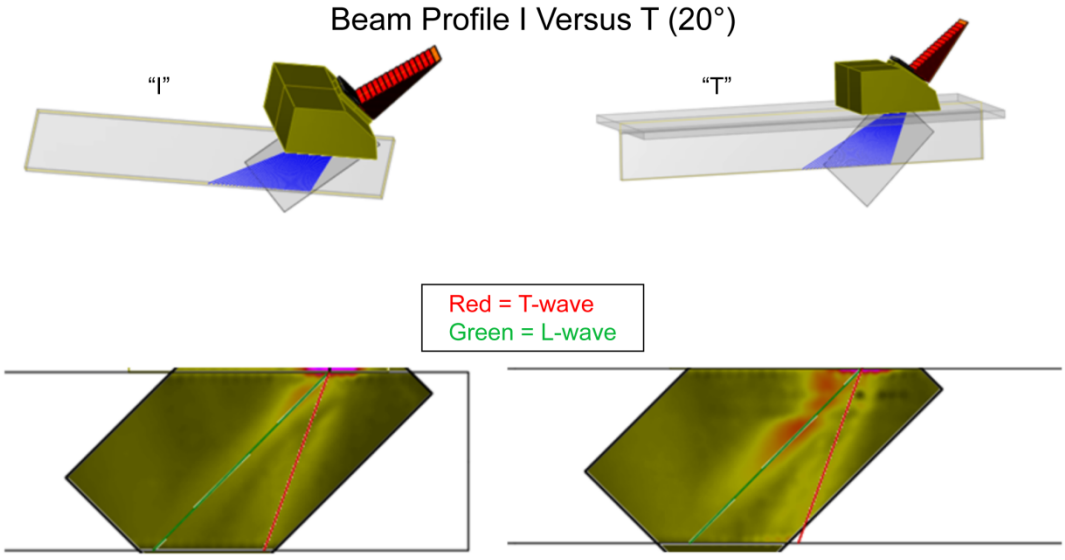

• Fillet of “T” solid model likely creates additional ultrasonic reflections

Figure 5.—Comparison of the beam profiles for the “I” and “T” solid models indicating some differences in resulting beams within the sample near the probe – sample interface.

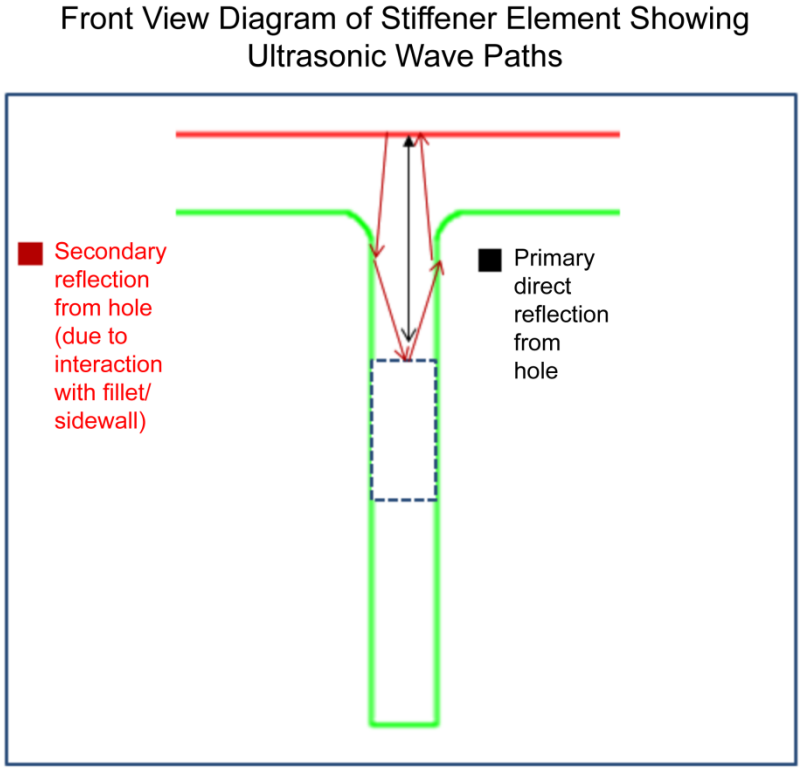

• Secondary reflection from hole (due to interaction with fillet/sidewall) will be missing from model in subsequent results since using “I” model.

Figure 6.—Wave paths with fillet present.

Flaw Response Experimental and Simulation Results

Figure 7 shows experimental and simulation results for the case where no flaws are emanating from a bolt hole (using "T" model for simulation since only flaw is bolt hole). Simulation shows the strong direct echo off of the bolt hole (an extension of the backwall) which agrees with experimental results. Angle of maximum amplitude is different by about 7° between simulation and experiment. Any slight differences in the setup, transducer model, and CAD model (including hole size and location) between simulation and experimentation would affect the angle (position) of max amplitude.

Figure 8 shows experimental and simulation results for examination of indications related to the bolt hole and downward-extending flaw (using "I" model for simulation since bolt hole and flaws are present). For the sector angle range 40° to 70°, only shear waves will be refracted in the part since the critical angle for longitudinal waves has been reached at 29.2° as was derived earlier (see Eq. (1)). In this case, four distinct corresponding echoes are identified in the experiment and simulation. The four corresponding echo indications are identified as that from the bolt hole, corner trap echoes related to the backwall – flaw – hole path (incomplete shadowing), flaw – backwall/backwall – flaw path, and backwall – hole path. Additionally, it is plausible that a creeping wave echo (Ref. 20) would be present at about the same time as shown for indication 2 and might be the primary indication for 2 in the experiment. Also, a fillet echo is likely present in the experimental results directly in line with indication 3 but slightly later in time in the experiment.

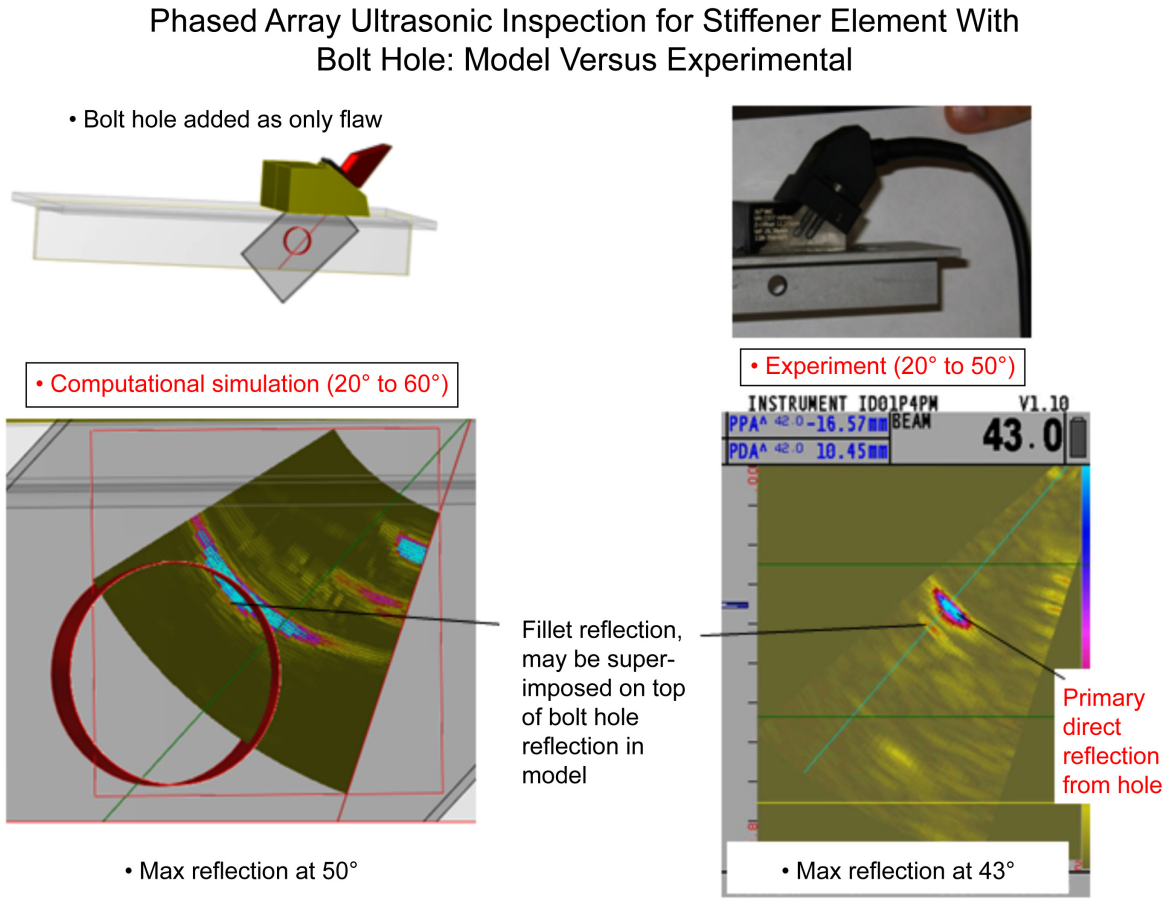

Figure 7.—Experimental and simulation results for the case where no flaws are emanating from the bolt hole. The "T" configuration can be used when the bolt hole is added as the only flaw.

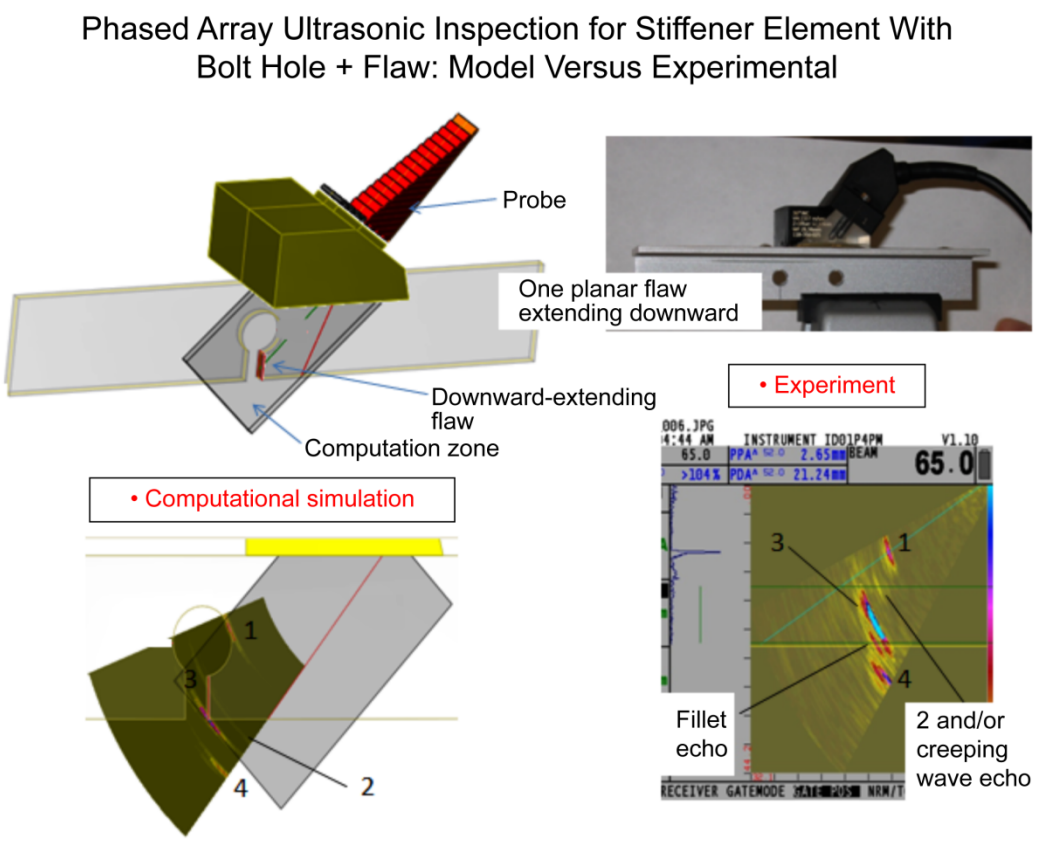

Figure 8.—Experimental and simulation results for the case where flaws extends downward from a bolt hole, probe is moved futher away from bolt hole as compared to case shown for just bolt hole (Fig. 6), and sector angle range changed to 40° to 70°. (Note: The “I” configuration must be used for the simulation as the bolt hole must be included as part of the original model back wall in order to model the backwall – flaw interaction properly. The downward-extending planar flaw (in red) extending from bolt hole on the model is not part of the hole itself but placed directly next to the downward extension of the hole that connects to the sample backwall.) Indications shown for both simulation and experiment: 1: Bolt hole echo; 2: Corner trap echo: backwall → flaw → hole; 3: Corner trap echo: flaw → backwall; 4: Corner trap echo: backwall → hole.

Figure 9 shows experimental and simulation results (reset for sector angle range 20° to 50°) for one flaw extending upward from the bolt hole at a 45° angle, one flaw extending downward, and with the probe position moved over the bolt hole so that examination of indications related to the bolt hole and upward-extending flaw could be examined. In this case, three distinct corresponding echoes are identified common to the experiment and simulation. These indications are for tip diffraction from the upper flaw, bolt hole reflection, and a corner trap echo related to the downward-extending flaw – backwall path. The backwall – hole path echo seen in Figure 7 is no longer present because the transducer has been moved over the bolt hole. To see the tip diffraction echo, the gain was adjusted higher in post-processing. Additionally, a possible creeping wave (Ref. 20) is identified for the experiment which travels around the bolt hole and is reflected at the intersection of the bolt hole and the downward-extending flaw. Again, a prominent fillet echo (indication 3) is likely present in the experimental results directly in line with indication 2 (echo from bolt hole) but slightly later in time in the experiment. This is not seen in the simulation since the fillet is not present in the "I" model.

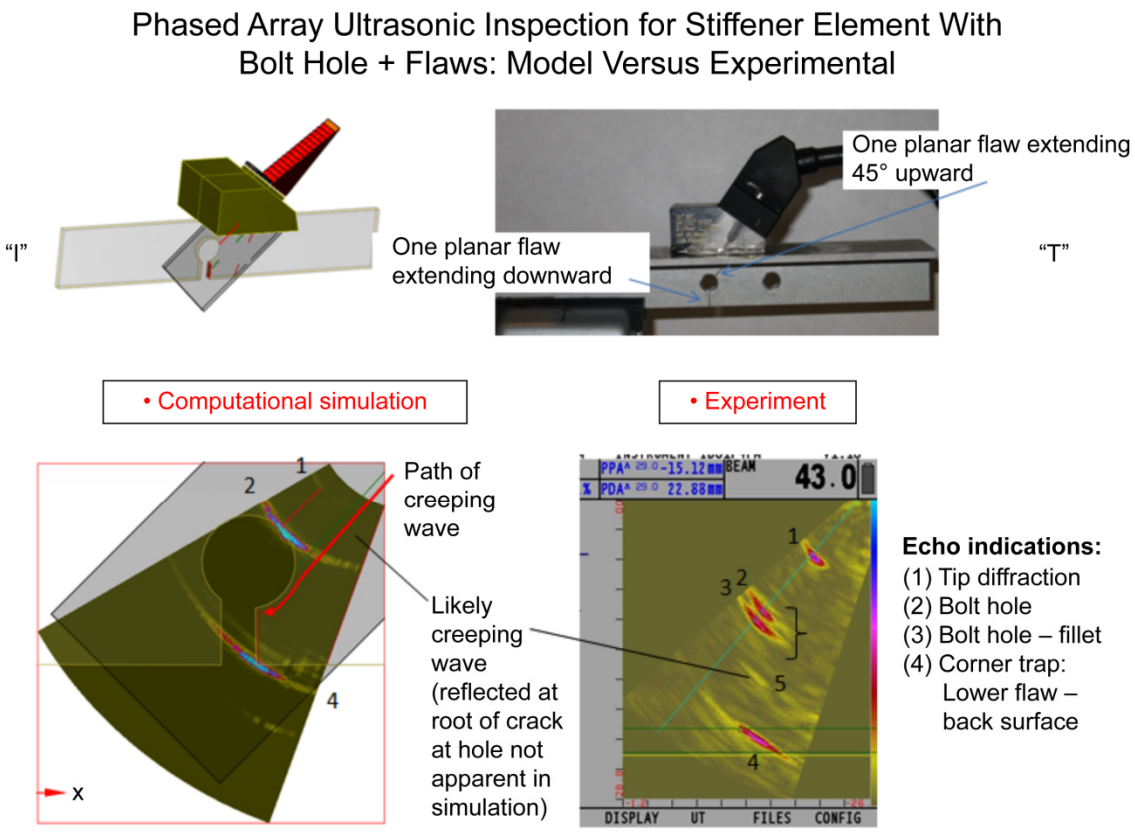

Figure 9.—Experimental and simulation results for the case where one flaw extends downward from a bolt hole and a second flaw extends upward from the bolt hole at 45° angle. The probe is moved closer to the bolt hole as compared to case shown for Figure 7, and sector angle range changed back to 20° to 50°. Indications shown for both simulation and experiment: 1: Tip diffraction; 2: Bolt hole; 3: Bolt hole → fillet; 4: Corner trap echo: backwall → downward-extending flaw; 5: Possible creeping wave.

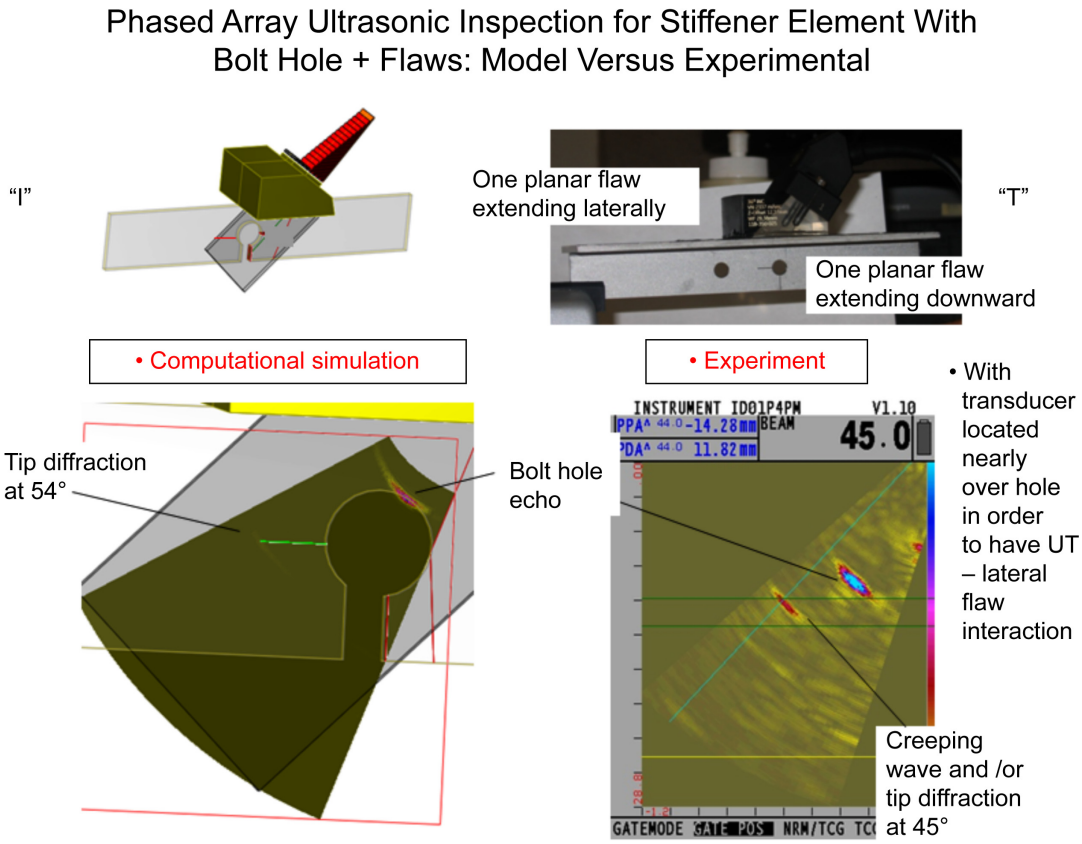

Figure 10.—Experimental and simulation results for the case where one flaw extends downward from a bolt hole and a second flaw extends laterally away from the bolt hole. Bolt hole, tip diffraction, and creeping wave indications seen experimentally. Tip diffraction indication is very faint on the simulation but is present and can be made more distinct by adjusting gain higher in post-processing in the CIVA software.

Figure 10 shows experimental and simulation results for the case where one flaw extends laterally (away from the probe) and one flaw extends downward from a bolt hole. The transducer has again been moved nearly directly over the bolt hole. Two echoes are common to the experiment and simulation. In addition to the bolt hole direct echo, a tip diffraction echo from the laterally-extending flaw is observed in both the simulation (very light indication) and experiment. It is also possible that the reflection from the laterally-extending flaw is due partially and possibly primarily to a creeping wave signal (Ref. 20) which will not be seen in the simulation. Tip diffraction echoes can be modeled correctly in CIVA with regards to their time-of-flight position, but not with respect to amplitude unless a calibration feature is utilized.

Conclusions and Future Efforts

This article describes experimental and simulation results for phased array ultrasonic inspection of an aluminum alloy isogrid stiffener element containing notches emanating from bolt holes. Good qualitative agreement was observed between experimental results and modeling predictions with regards to flaw response indications. The simulations were extremely important in helping to understand experimental results, even though the isogrid stiffener element solid model could not include the top section of the isogrid element for flaw response calculations. In a few cases, indications seen in the experimental results and expected from the simulation were not seen. The simulation software cannot currently model creeping waves, but future versions are being developed to address this limitation. The simulations compared well enough to the experimental results in a qualitative sense that the researchers would have

confidence in using them to predict significant inspection results. Future simulation work with isogrid stiffener element samples will be performed which examine other flaw configurations and in which CIVA batch processing capabilities are utilized to perform parametric studies. It would be interesting to vary flaw size, transducer frequency, and include material noise and attenuation in simulations in order to approximate limits of detectability for various inspection scenarios.

References

1. Isogrid Design Handbook - NASA CR-124075, Rev. A, Feb. 1973.
2. Atlas V Expendable Launch Vehicle (ELV) Rocket Propellant (RP)-1 Qualification Tank Failure Independent Assessment, NASA Engineering and Safety Center, RP-08-85, v1.1, August, 2008. ITAR-restricted document.
3. Moles, M.D.C. (Olympus NDT), Advances in Phased Array Ultrasonic Technology Applications, Olympus NDT, 2007.
4. Technical Focus Issue: Ultrasonic Phased Arrays, *Materials Evaluation*, vol. 65, no. 1, January 2007.
5. Roth, D.J., Tokars, R.P., Martin, R.E., Rauser, R.W., Aldrin, J.C., and Schumacher, E.J., Ultrasonic Phased Array Inspection Simulations of Welded Components at NASA, Materials Evaluation, vol. 67, no. 1, January 2009.
6. Mahaut S., Chatillon S., Kerbrat E., Porré J., Calmon P., and Roy O., "New features for phased array techniques inspections: simulation and experiments," 16th World Conf on Non Destructive Testing, Montréal, 2004.
7. Aldrin, J.C. and Knopp, J.S., "Modeling and Simulation for Nondestructive Testing With Applications to Aerospace Structures," *Materials Evaluation* vol. 66. no. 1 pp. 53–59 (2008).
8. Nondestructive Testing Handbook, Volume 7, Ultrasonic Testing, 2nd Ed., p. 49, 1991.
9. Roth, D.J., Kiser, J.D., Swickard, S.M., Szatmary, S., and Kerwin, D., "Quantitative Mapping of Pore Fraction Variations in Silicon Nitride Using an Ultrasonic Contact Scan Technique," *Research in Nondestructive Evaluation*, Volume 6, Number 3, 1995.
10. Achenbach, J.D., Wave propagation in Elastic Solids. Amsterdam, North Holland Publishing, 1973.
11. Achenbach, J.D., "Measurement Models for Quantitative Ultrasonics," *Journal of Sound and Vibration*, vol. 159, 1992, pp. 385–401.
12. Rose, J.L., Ultrasonic Waves in Solid Media. Cambridge, Cambridge University Press, 1999.
13. Gengembre N., "Pencil method for ultrasonic beam computation," Proc. of the 5th World Congress on Ultrasonics, Paris, 2003.
14. Raillon R. and Lecoeur-Taïbi I., "Transient elastodynamic model for beam flaw interaction. Application to nondestructive testing," *Ultrasonics*, 2000 38 527–530.
15. Darmon M., Calmon P. and Bele C., "Modeling of the ultrasonic response of inclusions in steels," in *Review of progress in QNDE*, vol. 22A, AIP publishing, 2003, pp. 101–108.
16. Lonne, S., de Roumilly, L., Le Ber, L., Mahaut, S. and Cattiaux, G., "Experimental Validation of CIVA Ultrasonic Simulations," International Conference on NDE in Nuclear Industry (ICNDE), 2006.
17. Cinquin, M., Le Ber, L., Lonne, S. and Mahaut, S., "Results of 2006 UT Modeling Benchmark Obtained with CIVA at CEA: Beam Modeling and Flaw Signal Prediction," in *Review of progress in QNDE*, vol. 26B, AIP publishing, 2007, pp. 1870–1877.
18. Chaffai-Gargouri, S., Chatillon, S., Mahaut, S. and Le Ber, L., "Simulation and Data Processing for Ultrasonic Phased-Arrays Applications," in *Review of progress in QNDE*, vol. 26A, AIP publishing, 2007, pp. 799–805.
19. Schmerr, L.W., Fundamentals of Ultrasonic Nondestructive Evaluation—A Modeling Approach. Plenum Press, New York, 1998.
20. Aldrin, J., Achenbach, J.D., Andrew, G., P'an, C., Grills, B., Mullis, R.T., Spencer, F.W., Golis, M., "Case Study for the Implementation of an Automated Ultrasonic Technique to Detect Fatigue Cracks in Aircraft Weep Holes," Materials Evaluation, vol. 59, no. 11, p. 1313, (2001).

REPORT DOCUMENTATION PAGE			Form Approved OMB No. 0704-0188

1. REPORT DATE *(DD-MM-YYYY)*	2. REPORT TYPE	3. DATES COVERED *(From - To)*
01-03-2010	Technical Memorandum	

4. TITLE AND SUBTITLE
Ultrasonic Phased Array Inspection for an Isogrid Structural Element With Cracks

5a. CONTRACT NUMBER

5b. GRANT NUMBER

5c. PROGRAM ELEMENT NUMBER

6. AUTHOR(S)
Roth, D., J.; Tokars, R., P.; Martin, R., E.; Rauser, R., W.; Aldrin, J., C.; Schumacher, E., J.

5d. PROJECT NUMBER

5e. TASK NUMBER

5f. WORK UNIT NUMBER
WBS 869021.03.03.01.08

7. PERFORMING ORGANIZATION NAME(S) AND ADDRESS(ES)
National Aeronautics and Space Administration
John H. Glenn Research Center at Lewis Field
Cleveland, Ohio 44135-3191

8. PERFORMING ORGANIZATION REPORT NUMBER
E-17135

9. SPONSORING/MONITORING AGENCY NAME(S) AND ADDRESS(ES)
National Aeronautics and Space Administration
Washington, DC 20546-0001

10. SPONSORING/MONITOR'S ACRONYM(S)
NASA

11. SPONSORING/MONITORING REPORT NUMBER
NASA/TM-2010-216090

12. DISTRIBUTION/AVAILABILITY STATEMENT
Unclassified-Unlimited
Subject Categories: 38 and 71
Available electronically at http://gltrs.grc.nasa.gov
This publication is available from the NASA Center for AeroSpace Information, 443-757-5802

13. SUPPLEMENTARY NOTES
Submitted to the Materials Evaluation

14. ABSTRACT
In this investigation, a T-shaped aluminum alloy isogrid stiffener element used in aerospace applications was inspected with ultrasonic phased array methods. The isogrid stiffener element had various crack configurations emanating from bolt holes. Computational simulation methods were used to mimic the experiments in order to help understand experimental results. The results of this study indicate that it is at least partly feasible to interrogate this type of geometry with the given flaw configurations using phased array ultrasonics. The simulation methods were critical in helping explain the experimental results and, with some limitation, can be used to predict inspection results.

15. SUBJECT TERMS
Nondestructive evaluation; Structures; Crack; Metal alloy; Stiffener element; Computational simulation; Ultrasonics; Isogrid; Modeling; Phased array

16. SECURITY CLASSIFICATION OF:			17. LIMITATION OF ABSTRACT	18. NUMBER OF PAGES	19a. NAME OF RESPONSIBLE PERSON
a. REPORT	b. ABSTRACT	c. THIS PAGE			STI Help Desk (email:help@sti.nasa.gov)
U	U	U	UU	18	19b. TELEPHONE NUMBER *(include area code)* 443-757-5802